Send Orders for Reprints to reprints@benthamscience.ae

The Open Mechanical Engineering Journal, **2014,** *8,* **765-769**

Open Access

Vehicle Side Crash Safety Research based on Dynamics Modeling and Analysis

Yao-Jun Zheng*

Zhejiang Technical Institute of Economics, HangZhou, Zhejiang, 310018, China

Abstract: The safety of vehicle side impact has become an important research content in the field of automotive passive safety. The nonlinear dynamic explicit finite element method is used to establish the side crashworthiness model of vehicle and side crash finite element model validation is also given. The finite element model is consistent with vehicle side stiffness, which can be used in the side crash simulation analysis. The simulation calculation and result analysis of side crash are carried out for a particular vehicle model to improve the side crash safety performance.

Keywords: Dynamics model, The finite element model, Vehicle side crash safety, Nonlinear dynamic explicit finite.

1. INTRODUCTION

With the rapid development of economy in our country, the car plays an increasingly important role in people's daily life. However, with the rapid increase in car ownership, it has also led to a variety of accidents and it not only has caused great damage to property, but also has caused a serious threat to people's life and safety. In all kinds of traffic accidents, the frontal crash and side impact have the highest frequency and the side impact is the form of accident with the highest occupant casualty rate. As a result, the safety of vehicle side impact study has become an important research content in the field of automotive passive safety [1].

System reliability design for vehicle crashworthiness and effects of various uncertainty reduction measures were proposed by Acar E [2]. Numerical simulations of multiple vehicle crashes and multidisciplinary crashworthiness optimization method were given by Fang H [3]. Improving accuracy of vehicle crashworthiness response predictions using ensemble of metamodels was also given by Acar E [4]. Automated vehicle structural crashworthiness design *via* a crash mode matching algorithm was proposed by Hamza K [5]. A two-stage multi-objective optimization method of vehicle crashworthiness under frontal impact was proposed by Liao XT [6]. Crashworthiness design optimization method of metal honeycomb energy absorber used in lunar lander was proposed by Li Meng [7]. Multi-objective optimization method of multi-cell sections for the crashworthiness design was proposed by Hou Shu-juan [8]. Optimizing crashworthiness design of square honeycomb structure was proposed by Meng Li [9]. A comparative study on multi-objective reliable and robust optimization for crashworthiness design of vehicle structure was given by Xianguang Gu [10], that took a typical vehicle structure subject to offset frontal crashing scenario as an example to compare reliable and robust designs with their deterministic counterpart. Multi-objective robust optimization method for crashworthiness during side impact was proposed by Sinha K [11]. Crashworthiness design of vehicle by using multi-objective robust optimization was proposed by Sun GY [12]. Crushing analysis and multi-objective crashworthiness optimization of honeycomb-filled single and bitubular polygonal tubes were given by Yin HF [13].(Repeated sentence) Structural and Multidisciplinary Optimization was proposed by Guangyong Sun [14]. Automotive crashworthyness design using response surface-based variable screening and optimization was proposed by Craig KJ [15]. A method for selecting surrogate models in crashworthiness optimization was proposed by Lei Shi [16]. Probability-based least square support vector regression meta modeling technique for crashworthiness optimization problems was proposed by Hu Wang [17]. Multipoint version of space mapping optimization applied to vehicle crashworthiness design was proposed by Redhe M [18].

In the next section, the nonlinear dynamic explicit finite element method is investigated. In Section 3, side crash finite element model validation is given. In section 4, the simulation calculation and result analysis of side crash are given. Finally, some conclusions are presented in section 5.

2. THE NONLINEAR DYNAMIC EXPLICIT FINITE ELEMENT METHOD

Vehicle crash is a very complex dynamic problem. In the process of vehicle crash, the crash process has highly nonlinear property, such as geometric nonlinearity, material nonlinearity and contact nonlinearity etc., so choosing a suitable calculation theory for vehicle crash simulation analysis is particularly important. In the vehicle crash simulation analysis, the numerical simulation methods are mainly multi-rigid body dynamics research method and nonlinear dynamic display finite element method. The former mainly studies the response of human body and vehicle parts. This paper mainly studies vehicle side crashworthiness and the nonlinear dynamic display finite

Address correspondence to this author at the Zhejiang Technical Institute of Economics, HangZhou, Zhejiang, China; E-mail: zhengyaojun@126.com

1874-155X/14

element method is used for vehicle crash simulation and analysis.

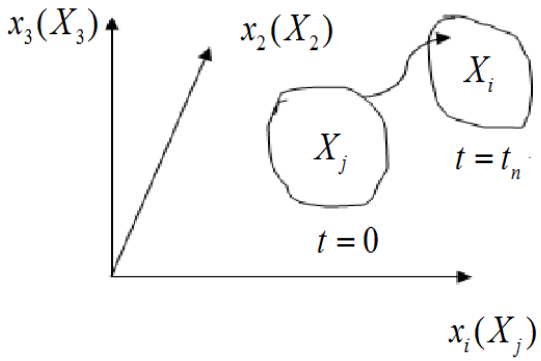

Fig. (1). Movement of particle.

The movement of particle is shown in Fig. (**1**). At initial time, the coordinates of the particle are $X_i(i=1,2,3)$. The coordinates of the particle at any time t are $x_i(i=1,2,3)$, and the movement equation of the particle is $x_i = x_i(X_j,t)$. The initial condition at time 0 is $x_i(X_j,0)=X_j$, $x_i(X_j,0)=V_i(X_j,0)$.

V_i represents the initial speed. The momentum conservation equation is $\delta_{ij,j}+\rho f_i = \rho\overline{x_i}$.

δ_{ij} represents Cauchy stress, $\delta_{ij,j}=\dfrac{\partial\delta_{ij}}{\partial x_j}$, f_i represents unit mass volume force, $\overline{x_i}$ represents acceleration and ρ represents mass density. The mass conservation equation is $\rho = J\rho_0$.

ρ_0 represents mass density at initial time and J represents change coefficient of system density. Energy conservation equation is $E = V\delta_{ij}\dot{\varepsilon}_{ij}-(p+q)V$.

This equation is used for calculation of state equation and the overall energy balance. V represents the volume of the current configuration, $\dot{\varepsilon}_{ij}$ represents strain rate tensor, p represents pressure and q represents volume viscous resistance. The boundary condition of surface force s^1 is $\delta_{ij}n_j = T_i(t)$.

$n_j(j=1,2,3)$ represents direction cosine of the outward normal, $T_i(i=1,2,3)$ represents the surface force load. The boundary condition of s^2 displacement is $X_i(X_i,t)=K_i(t)$.

$K_i(t)$, $i=1,2,3$ represent the known displacement linear function. Specific algorithm of the explicit integral algorithm is as follows.

The dynamics equilibrium equation is

$$\ddot{u}_{(t)} = M^{-1}\cdot(P_{(t)}-I_{(t)}).$$

The explicit integral of time is

$$\dot{u}_{(t+\frac{\Delta t}{2})} = \dot{u}_{(t-\frac{\Delta t}{2})} + \frac{(\Delta t_{(t+\Delta t)}+\Delta t_{(t)})}{2}\ddot{u}_t .$$

$$u_{(t+\Delta t)} = u_{(t)} + \Delta t_{(t+\Delta t)}\dot{u}_{(t+\frac{\Delta t}{2})} .$$

According to the strain rate $\dot{\varepsilon}$, cell strain increment $d\varepsilon$ is calculated. According to the constitutive relation, stress σ, $\sigma_{(t+\Delta t)} = f(\sigma_{(t)},d\varepsilon)$ is calculated. Integrated node internal force is $I_{(t+\Delta t)}$.

The explicit central difference method is stable, only when the time step is less than the critical time step

$$\Delta t \le \Delta t_{crit} = \frac{2}{w_{\max}} .$$

$w_{\max}$ represents the maximum angular frequency. Because the natural frequency of bar, $w_{\max} = 2\dfrac{c}{l}$. Critical time step of the bar is

$\Delta t = \dfrac{l}{c}$, l and c is determined by unit type. For quadrilateral shell element, $l = \dfrac{A}{\max(L_1,L_2,L_3,L_4)}$.

For triangular shell element, $l = \dfrac{2A}{\max(L_1,L_2,L_3)}$, $c = \sqrt{\dfrac{E}{\rho(1-v^2)}}$.

Due to the constant material properties, the time step is completely determined by unit minimum size. The smaller the cell size, the smaller the time step is and more computing resources and cost are required. When the finite element model is established, it is important to note that the minimum cell size is required.

3. SIDE CRASH FINITE ELEMENT MODEL VALIDATION

According to GB 20071-2006 regulations, the side crash simulation model is established as shown in Fig. (**2**). Mobile deformation wall vertically crashes the side of the static vehicle at a speed of 50 km/h, its perpendicular bisector crashes side front seat through vehicle, and simulation time is 140 ms. The systems' overall energy change is shown in Fig. (**3**). The top green line represents total energy, the middle green line represents kinetic energy of the system, the middle red line represents internal energy, the bottom red line represents interface energy and the blue line represents hourglass energy. The horizon axis represents time, the unit of which is millisecond and the vertical axis represents

energy. The sliding interface energy and the hourglass energy can keep small positive value, which is no more than 5% of the total energy. Fig. (**4**) is the acceleration-time curve of the bottom B-pillar of the bumped side. The blue line represents simulation and the red line represents experiment. The figure shows that change trend of the acceleration curve is almost the same, and peak value and turning up time are in good agreement. The existence of the error may be due to the omitted vehicle accessories, material parameters and soldered dots, but the overall error is less than 5%. The finite element model is consistent with vehicle side stiffness which can be used in the side crash simulation analysis.

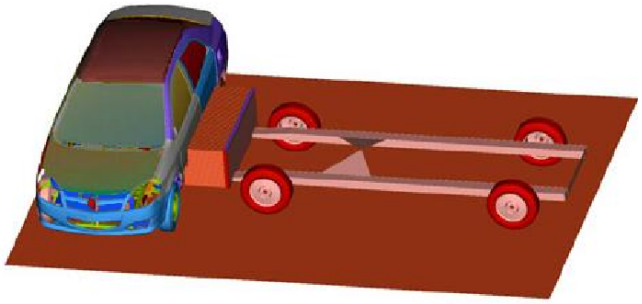

Fig. (2). Vehicle side crash model.

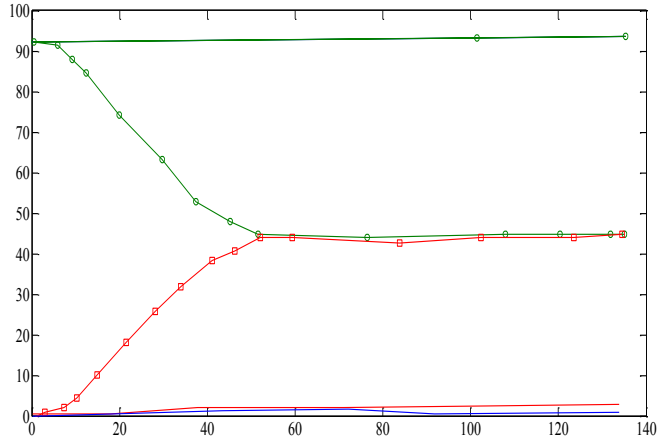

Fig. (3). Overall energy curve.

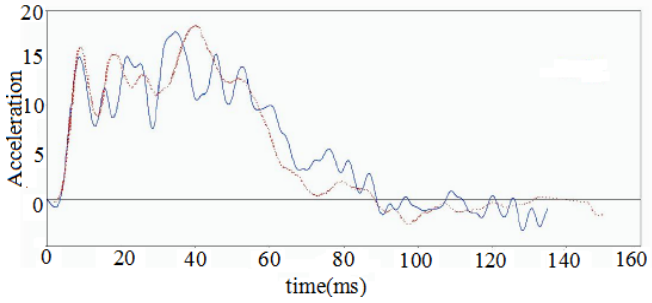

Fig. (4). The acceleration-time curve of the bottom B-pillar of the bumped side.

4. SIMULATION AND ANALYSIS OF SIDE CRASH

A particular vehicle model is taken as researched object. Inside of the door plank of the left front door can damage dummy people included in the experiment. The research results show that the relation between chest damage value and intrusion velocity is

$$TTI = 60.60 - 0.03M + 0.93V_d - 0.12a_d + 0.70C_d .$$

Relation between damage value at pelvis location and intrusion quantity is

$$a_p = -19.1 - 0.05m + 2.02C_d + 0.04L - 0.10a_d .$$

TTI represents chest injury index, m represents vehicle quality, V_d represents maximum intrusion speed V for the door. a_p represents pelvis acceleration, C_d represents maximum intrusion quantity of door, L represents wheelbase and a_d represents maximum acceleration of door of vehicle. The maximum intrusion quantity and maximum intrusion speed can damage people greatly. In Fig. (**5**), P and Q point to crash contact area related to the chest and the pelvis. R points to biggest position area of B pillar deformation. Intrusion quantity and intrusion speed of three positions are shown in Table **1**. Reducing the intrusion capacity and speed index of the three positions can improve the body energy absorbing structure to improve side impact safety performance. If intrusion quantity and intrusion velocity are small, the side impact safety is higher. Roof longitudinal beam deformation is shown in Fig. (**6**), vehicle side crash deformation is shown in Fig. (**7**), vehicle threshold deformation is shown in Fig. (**8**) and side surround deformation is shown in Fig. (**9**).

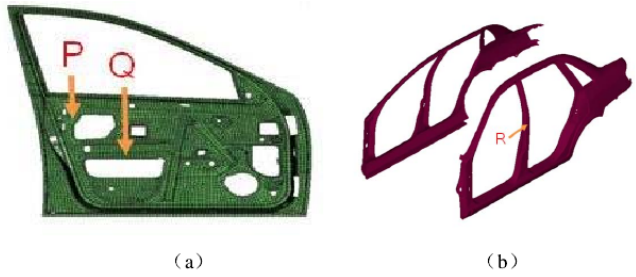

Fig. (5). P,Q,R position.

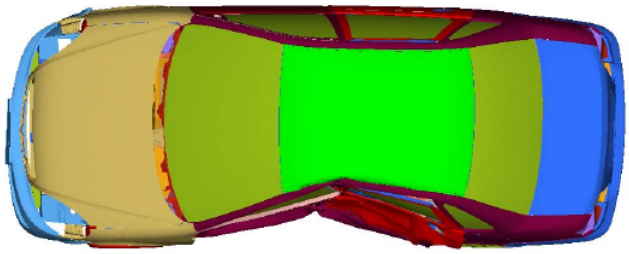

Fig. (6). Roof longitudinal beam deformation.

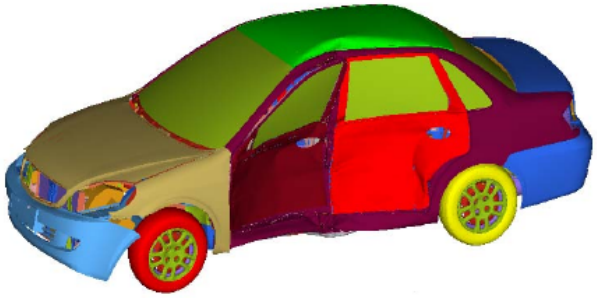

Fig. (7). Vehicle side crash deformation.

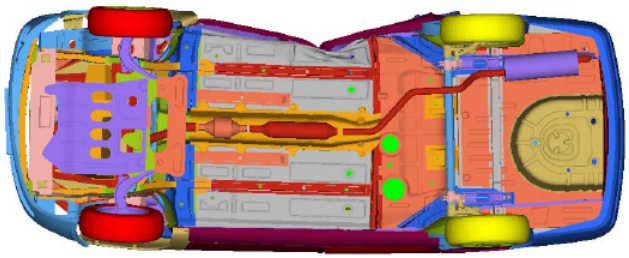

Fig. (8). Vehicle threshold deformation.

Fig. (9). Side surround deformation.

Table 1. Intrusion quantity and intrusion speed of three positions.

Position	Intrusion Quantity (mm)	Intrusion Speed (mm/ms)
P	330	15.5
Q	300	14.5
R	340	13.8

The intrusion quantity and speed of this vehicle are large, which cause serious damage to people's life and safety. Connection parts between B-pillar and the roof left side longitudinal beam and the threshold step have serious deformation. Stiffness of central parts of B-pillar is too weak which causes the intrusion quantity and speed of P, Q and R to become greater. Velocity curve of the B-pillar is shown in Fig. (**10**) and the door velocity curve is shown in Fig. (**11**).

After the crash of 20 ms, B-pillar crash speed changes gently. After the crash of 32 ms, the speed achieves the peak value 9.6 m/s. After 70 ms, it gradually achieves a more stable speed. From Fig. (**11**), it can be seen that at about 40 ms, the speed achieves the peak value 14.7 m/s, which takes place within a few milliseconds after the crash has just started. There is only 20 to 30 centimetres distance between the people and the door, so the crash impact is bigger.

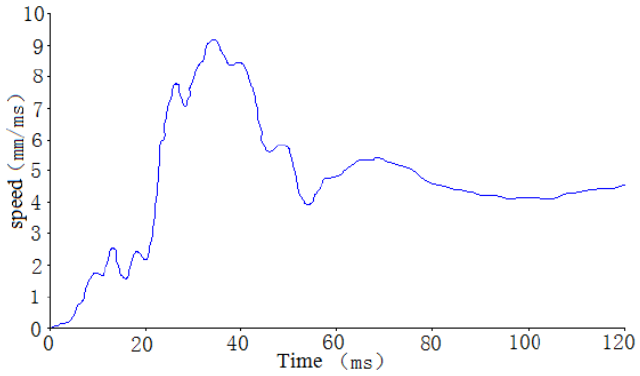

Fig. (10). Velocity curve of the B-pillar.

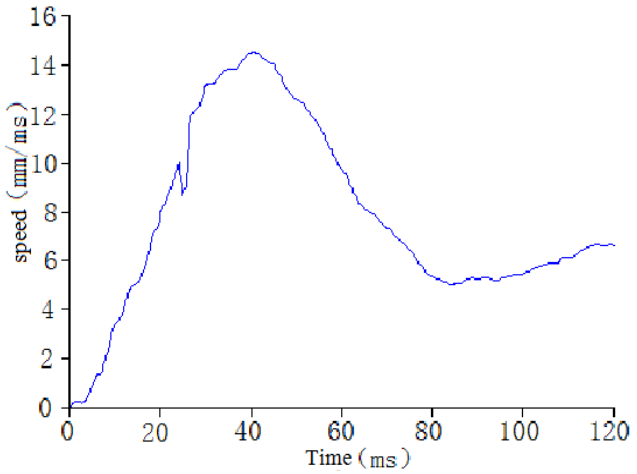

Fig. (11). Door velocity curve.

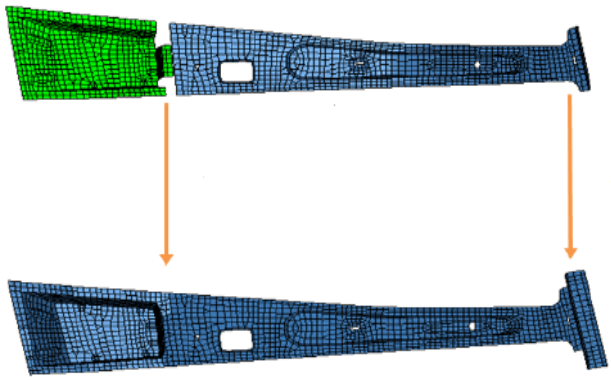

Fig. (12). Structure comparison of B-pillar before and after optimization.

CONCLUSION

It can be concluded that some principles have been proposed to improve side crashworthiness of vehicle. B-pillar buckling deformation and excessive varus deformation should not occur. Structure comparison of B-pillar before

and after optimization is shown in Fig. (**12**) and the crash effect after improvement of B-pillar is shown in Fig. (**13**).

Fig. (13). The crash effect after improvement of B-pillar.

The anti-collision board inside the door has enough stiffness and it does not produce too much bending deformation. Top beam and stringer connected with B-pillar must have enough stiffness and buckling deformation and excessive varus deformation should not occur. Floor beam should have enough stiffness and force transmission capability. The door threshold has larger contact area with the lower edge to reduce the intrusion of the door. The maximum deformation position of B-pillar is at the bottom as far as possible.

CONFLICT OF INTEREST

The author confirms that this article content has no conflict of interest.

ACKNOWLEDGEMENTS

This work is supported by the Science and Technology Department of Zhejiang Province in 2013 project "Internet based specialty car simulation training platform to build" (NO. 2013C31077).

REFERENCES

[1] H. Kurtaran, A. Eskandarian, D. Marzougui, and N.E. Bedewi, "Crashworthiness design optimization using successive response surface approximations", *Computational Mechanics*, vol. 29, no. 4-5, pp. 409-421, 2002.

[2] E. Acar, and K.N. Solanki, "System reliability based vehicle design for crashworthiness and effects of various uncertainty reduction measures", *Structural and Multidisciplinary Optimization*, vol. 39, no. 3, pp. 311-325, 2009.

[3] H. Fang, K.N. Solanki, and M.F. Horstemeyer, "Numerical simulations of multiple vehicle crashes and multidisciplinary crashworthiness optimization", *International Journal of Crashworthiness*, vol. 10, no. 2, pp. 161-171, 2004.

[4] E. Acar, and K.N. Solanki, "Improving accuracy of vehicle crashworth-iness response predictions using ensemble of metamodels", *International Journal of Crashworthiness*, vol. 14, no. 1, pp. 49-61, 2009.

[5] K. Hamza, and K. Saitou, "Automated vehicle structural crashworthiness design *via* a crash mode matching algorithm. Transactions of ASME", *Journal of Mechanical Design*, vol. 133, no. 1, pp. 011003-1-011003-9, 2011.

[6] X.T. Liao, Q. Li, X.J. Yang, W. Li, and W.G. Zhang, "A two-stage multi-objective optimisation of vehicle crashworthiness under frontal impact", *International Journal of Crashworthiness*, vol. 13, no. 3, pp. 279-288, 2008.

[7] M. Li, Z. Deng, R. Liu, and H. Guo, "Crashworthiness design optimisation of metal honeycomb energy absorber used in lunar lander", *International Journal of Crashworthiness*, vol. 16, no. 4, pp. 411-419, 2011.

[8] S. Hou, Q. Li, S. Long, X. Yang, and W. Li, "Multiobjective optimization of multi-cell sections for the crashworthiness design", *International Journal of Impact Engineering*, vol. 35, no. 11, pp. 1355-1367, 2008.

[9] M. Li, Z. Deng, H. Guo, R. Liu, and B. Ding, "Optimizing crashworthiness design of square honeycomb structure", *Journal of Central South University*, vol. 21, no. 3, pp. 912-919, 2014.

[10] X. Gu, G. Sun, G. Li, L. Mao, and Q. Li, "A Comparative study on multiobjective reliable and robust optimization for crashworthiness design of vehicle structure", *Structural and Multidisciplinary Optimization*, vol. 48, no. 3, pp. 669-684, 2013.

[11] K. Sinha, R. Krishnan, and D. Raghavendra, "Multiobjective robust optimisation for crashworthiness during side impact", *International Journal of Vehicle Design*, vol. 43, nos. 1-4, pp. 116-135, 2007.

[12] G.Y. Sun, G.Y. Li, S.W. Zhou, H.Z. Li, S.J. Hou, and Q. Li, "Crashworthiness design of vehicle by using multiobjective robust optimization", *Structural and Multidisciplinary Optimization*, vol. 44, no. 1, pp. 99-110, 2011.

[13] H.F. Yin, G.L. Wen, S.J. Hou, and K. Chen, "Crushing analysis and multiobjective crashworthiness optimization of honeycomb-filled single and bitubular polygonal tubes", *Materials & Design*, vol. 32, no. 8-9, pp. 4449-4460, 2011.

[14] G. Sun, G. Li, S. Zhou, H. Li, S. Hou, and Q. Li, "Crashworthiness design of vehicle by using multiobjective robust optimization", *Structural and Multidisciplinary Optimization*, vol. 44, no. 1, pp. 99-110, 2011.

[15] K.J. Craig, N. Stander, D.A. Dooge, and S. Varadappa, "Automotive crashworthiness design using response surface-based variable screening and optimization", *Engineering Computations*, vol. 22, no. 1-2, pp. 38-61, 2005.

[16] L. Shi, R.J. Yang, and P. Zhu, "A method for selecting surrogate models in crashworthiness optimization", *Structural and Multidisciplinary Optimization*, vol. 46, no. 2, pp. 159-170, 2012.

[17] H. Wang, E. Li, and G.Y. Li., "Probability-based least square support vector regression metamodeling technique for crashworthiness optimization problems", *Computational Mechanics*, vol. 47, no. 3, pp. 251-263, 2011.

[18] M. Redhe, and L.A. Nilsson, "Multipoint version of space mapping optimization applied to vehicle crashworthiness design", *Structural and Multidisciplinary Optimization*, vol. 31, no. 2, pp. 134-146, 2006.

Received: December 8, 2014 Revised: December 15, 2014 Accepted: December 16, 2014